COMPUTATION OF IMPULSE INITIATION AND SALTATORY CONDUCTION IN A MYELINATED NERVE FIBER

RICHARD FITZHUGH
From the National Institutes of Health, Bethesda

ABSTRACT A mathematical model of the electrical properties of a myelinated nerve fiber is given, consisting of the Hodgkin-Huxley ordinary differential equations to represent the membrane at the nodes of Ranvier, and a partial differential cable equation to represent the internodes. Digital computer solutions of these equations show an impulse arising at a stimulating electrode and being propagated away, approaching a constant velocity. Action potential curves plotted against distance show discontinuities in slope, proportional to the nodal action currents, at the nodes. Action potential curves plotted against time, at the nodes and in the internodes, show a marked difference in steepness of the rising phase, but little difference in peak height. These results and computed action current curves agree fairly accurately with published experimental data from frog and toad fibers.

INTRODUCTION

Hodgkin and Huxley's set of ordinary differential equations for the squid giant nerve fiber membrane has previously been solved for the case of a space clamp, in which the potential, current, and other variables of state of the membrane vary with time but not with distance along the fiber (Hodgkin and Huxley, 1952; Cole, Antosiewicz, and Rabinowitz, 1955; FitzHugh and Antosiewicz, 1959; FitzHugh, 1960; George, 1960; FitzHugh, 1961). Cases in which these variables vary with distance as well as with time are described by the partial differential equation of Hodgkin and Huxley, which is a cable equation with a distributed Hodgkin-Huxley (HH) membrane instead of the usual passive resistive layer. By assuming propagation of fixed wave forms for all state variables at a constant velocity along the fiber, Hodgkin and Huxley reduced this partial differential equation to an ordinary differential equation, solutions of which are given in several of the above references (also Huxley, 1959*a*, 1959*b*). The mathematical description of the growth of an impulse and its subsequent propagation away from a stimulating electrode, however, still requires the solution of the full partial differential equation.

The estimated time required to solve the HH partial differential equation with an IBM 704 digital computer was too high to make such solutions practical, because for each instant of time the HH ordinary equations must be solved at a large number of points along the fiber (using the usual difference equation approximation to the differential equation, with small enough distance increments for reasonable accuracy). The case of a myelinated fiber is better suited to computation. The nodes of Ranvier can be represented as active point sources of current evenly spaced along a one-dimensional x-axis and separated by sections of passive electrical cable representing the internodes (Huxley and Stämpfli, 1949). This case requires that the active membrane equations be solved at far fewer points along the fiber (at the nodes only) than does the case of a continuous axon.

The HH equations were considered adequate to represent the membranes at the nodes, at least qualitatively, because of the resemblance between the nodal currents recorded under potential clamp by Dodge and Frankenhaeuser (1958) and those in squid. The model used here may actually deliver rather more current than the frog node (see below). Different equations are now available, designed for the frog node by Dodge (1961), and they would be better for future computations of this sort than the equations used here. Nevertheless, these computations establish the existence of a pair of impulses which arise at the stimulating electrode and are propagated away at a constant velocity in both directions, agreeing fairly well with experimental measurements on frog and toad myelinated axons.

EQUATIONS

Fig. 1 shows the equivalent circuit of the fiber. There is a Ranvier node at the origin ($x = 0$), and the others are evenly spaced at an internodal distance of 2 mm. By assuming symmetry about the origin in x, only non-negative values of x need be considered. Stimulating current flows to the axon at the origin through an electrode. The electrical circuit is completed by electrodes at plus and minus infinity in x.

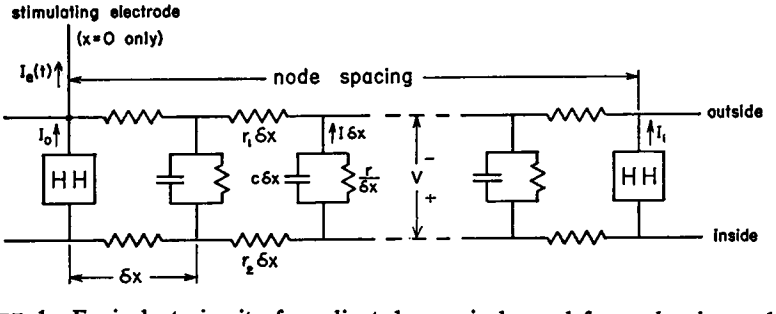

FIGURE 1 Equivalent circuit of myelinated axon in lumped form, showing nodes 0 and 1 with increments δx as used in difference equation solved by computer. HH indicates Hodgkin-Huxley membrane model at nodes of Ranvier. Myelin between nodes is represented by passive RC circuits to approximate a distributed leaky cable.

The equations are shown below. (1) is the cable differential equation for the potential across the myelin layer in the internodes. (2) to (5) are the HH differential equations for the membrane potential and the three conductance variables at the jth node ($j = 0, 1, 2, 3, \ldots$), at $x = 2j$ mm. (6) expresses the continuity of potential at the nodes. (7) and (8) are the boundary conditions at the nodes for equations (1). (9) gives the initial conditions (uniform resting state). (10) or (11) describes the wave form (brief pulse or step) of the stimulating electrode current. The 2 in equation (7) results from adding the left and right derivatives of V at $x = 0$, which are equal in magnitude because of symmetry.

TABLE I

Variables
t = time (msec.)
x = distance along axon (mm)
  jth node: $x = 2j$ mm, $j = 0, 1, 2, 3, \ldots\ldots$
  jth internode: $2(j-1)$ mm $< x < 2j$ mm
$V(x, t)$ = potential difference across myelin sheath in internodes, inside minus outside (mv)
$I(x, t)$ = outward current density across myelin (μa/mm)
$V_j(t)$ = membrane potential difference at jth node (mv)
$m_j(t)$, $h_j(t)$, $n_j(t)$ = HH conductance variables at jth node (dimensionless)
$I_j(t)$ = outward membrane current at jth node (μa)
$I_e(t)$ = stimulating current through electrode at $x = 0$ (μa)
I_p = amplitude of rectangular pulse (0.01 msec. duration), or step, of $I_e(t)$
Constants
$r_1 + r_2$ = total longitudinal resistance = 15 Megohm/mm (Tasaki and Frank, 1955, p. 573)
c = myelin capacitance = 1.6 $\mu\mu$f/mm (Tasaki, 1955, p. 648)
r = myelin resistance = 290 Megohm mm (Tasaki, 1955, p. 643)
C_N = nodal membrane capacitance = 1.5 $\mu\mu$f (Tasaki, 1955, p. 645)
A = area of HH membrane at each node = 0.003 mm^2 (see text)
L = node spacing = 2 mm

Table I gives definitions of the symbols and values of the constants, with literature references to the sources used.

$$c\,\partial V/\partial t = (\partial^2 V/\partial x^2)/(r_1 + r_2) - V/r \tag{1}$$

$$C_N\,dV_j/dt = I_j - A[\bar{g}_{Na} m_j^3 h_j (V_j - V_{Na}) + \bar{g}_K n_j^4 (V - V_K) + \bar{g}_L (V_j - V_L)] \tag{2}$$

$$dm_j/dt = (1 - m_j)\alpha_m(-V_j) - m_j\beta_m(-V_j) \tag{3}$$

$$dh_j/dt = (1 - h_j)\alpha_h(-V_j) - h_j\beta_h(-V_j) \tag{4}$$

$$dn_j/dt = (1 - n_j)\alpha_n(-V_j) - n_j\beta_n(-V_j) \tag{5}$$

$$\lim_{x \to jL} V(x, t) = V_j(t); \qquad j = 0, 1, 2, 3, \cdots \tag{6}$$

$$I_0 = (r_1 I_e + 2 \lim_{x \to 0} \partial V/\partial x)/(r_1 + r_2) \tag{7}$$

$$I_j = (\lim_{x \to jL+0} \partial V/\partial x - \lim_{x \to jL-0} \partial V/\partial x)/(r_1 + r_2) \tag{8}$$

$$\left.\begin{aligned} V_j(0) &= V(x, 0) = 0; \quad \text{all} \quad x \\ m_j(0) &= m_\infty(0) = \alpha_m(0)/[\alpha_m(0) + \beta_m(0)] \\ h_j(0) &= h_\infty(0) = \alpha_h(0)/[\alpha_h(0) + \beta_h(0)] \\ n_j(0) &= n_\infty(0) = \alpha_n(0)/[\alpha_n(0) + \beta_n(0)] \end{aligned}\right\} \tag{9}$$

$$I_s(t) = \begin{cases} I_p; & 0 \leq t \leq 0.01 \text{ msec.} \\ 0; & 0.01 \text{ msec.} < t \end{cases} \tag{10}$$

$$I_s(t) = I_p; \quad 0 \leq t \tag{11}$$

To agree with present practice, the variables for potential and current have been taken with the signs reversed from those used by Hodgkin and Huxley (1952). V and V_j represent potential difference—inside minus outside—and currents I and I_j are positive outward. Hence the minus signs before the arguments of the α and β functions. These functions are given by Hodgkin and Huxley (1952).

Since in the HH equations membrane current and conductance are expressed per cm^2 of membrane area, a suitable area A of theoretical HH membrane must be chosen to give nodal currents of proper magnitude. At the start of these computations, experimental measurements of nodal membrane capacitance and resting conductance were available for this purpose. Since the node has a much smaller capacitance relative to its resting conductance than the squid axon, it was decided to match the conductance and to decrease the HH capacitance value. This was the only modification of the HH equations made.

The area A of theoretical HH membrane was chosen to be 0.003 mm^2, in order to provide the correct resting conductance. This value, when multiplied by the HH resting conductance of 6.77 μmho/mm^2, gives 0.02 μmho, which is the resting conductance of the node as measured by Tasaki and Freygang (1955, p. 216) and Tasaki (1955, p. 645). Notice that A is not intended to be the actual area of the nodal membrane (which may be quite different), but is only a scale factor to adjust the nodal currents.

In a paper which appeared after the present computations were begun, Dodge and Frankenhaeuser (1958) measured maximum peak nodal current under potential clamp in frog nodes which had been made more potent by a previous hyperpolarizing pulse. Their value appears to be about equal to those to be expected from the present equations. (However, their currents are expressed in ma/cm^2, with only approximate data on the actual area for the node.) A node without previous hyperpolarization, as used in normal propagation experiments, gives maximum peak currents only about half their value (Dodge, personal communication).

The nodal membrane capacitance C_N is taken as 1.5 $\mu\mu$f, as measured by Tasaki

(1955). This is only one-twentieth of the capacitance of an area A of the original HH membrane, which has a capacitance of 1.0 μf/cm^2.

Hodgkin and Huxley's standard temperature of 6.3°C was used.

In equation (7), the stimulating current appears in the term $r_1 I_e/(r_1 + r_2)$, which may be thought of as the "effective stimulating current." The corresponding amplitudes $r_1 I_p/(r_1 + r_2)$, which were specified in the computations, are given in Table II. Only the value of $r_1 + r_2$ was specified in the computations (Table I). However, r_1 was assumed to be small relative to r_2, and $r_1 + r_2$ was therefore taken to be equal to the experimentally measured value of axoplasmic resistance (Table I). Using this value and any assumed small value of r_1, one could calculate I_p from the values in the table. All values of stimulating current are positive and therefore outward or cathodal.

COMPUTING METHOD

The partial differential equations were replaced in the usual way by difference equations (Milne, 1953; Scarborough, 1958) with space and time increments $\delta x = 0.25$ mm and $\delta t = 0.00075$ msec. The results were printed out at intervals of δx and $32\delta t$ (= 0.024 msec.) The smallness of δx and the size of the (x, t) domain of integration are limited by the time and expense of computer runs. For a given δx, δt must be chosen small enough to insure computational stability. The principle involved in insuring stability is similar to that for the one-dimensional heat flow equation as described by Milne (1953). Each computer solution took 1½ hours on the IBM 704 for the following domain of integration: $x = 0$ to 26.75 mm, $t = 0$ to 1.392 msec. This domain was too small to permit the computation of complete action potential curves; the longest ones stop after the peak, less than half way down the descending phase (Figs. 2, 3).

Although the fiber goes to infinity in x, the computation was necessarily performed over a finite x interval. Since the computation of the dependent variables at $t + \delta t$ and x depends on their values at t and $x \pm \delta x$, the x interval of computation had to be shortened by δx at its right end for each advance in t, and the starting x interval at $t = 0$ had to be much longer than the above mentioned figure of 26.75 mm. On the other hand, some computation time was saved by the fact that the first departure of the dependent variables from their initial resting values progressed along the x axis at a finite velocity equal to $\delta x/\delta t$. At any $x > 0$, therefore, no values needed to be computed for $t \leq x(\delta t/\delta x)$. The actual domain of computation in the (x, t) plane was a quadrilateral determined by these conditions, but values were printed out only for the rectangular region mentioned above.

To check the effect of increment size, one run was made with $\delta x = 0.20$ mm and $\delta t = 0.00048$ msec. The domain of integration in t had to be decreased to 1.032 msec. The conduction velocity was unchanged. The values of membrane potential V at the nodes at corresponding times differed by only 0.004 mv at the peak of a tem-

poral action potential curve, but by as much as 2 mv elsewhere. However, the two plotted curves could be brought into close agreement by shifting one of them along the time axis by about 0.005 msec., which shows that the principal result of decreasing the increment size was to increase the latency slightly, leaving the form of the action potential otherwise unchanged. Since extreme accuracy was not required, no further tests of changing increment size were made.

RESULTS

Fig. 2 shows computed *spatial* action potential curves (V plotted against x) at different instants of time as the impulse travels away from the origin. Each curve has a cusp at each node. The discontinuity in slope at each cusp is proportional to the

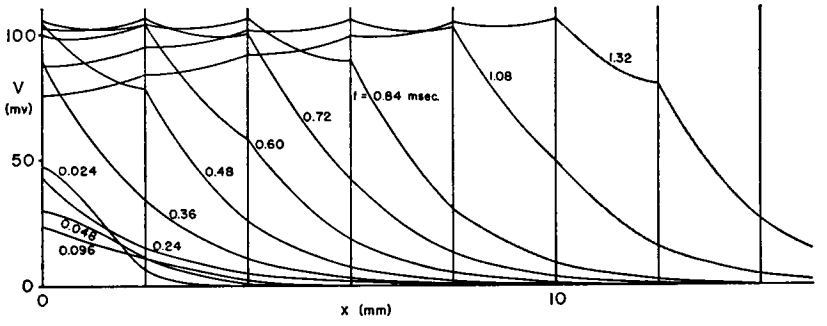

FIGURE 2 Spatial action potential curves following stimulation by a 30,000 μa pulse of 0.01 msec. duration beginning at $t = 0$. Each curve corresponds to one value of t as labeled. The impulse arises at $x = 0$ (location of stimulating electrode) and is propagated away at a constant velocity. Solutions are symmetric about the origin; therefore the negative x-axis is not shown. Vertical lines indicate node positions. Each curve is drawn through the computed points, 8 per internode (0.25 mm spacing).

nodal membrane current according to equation (8). A similar curve was reconstructed by Huxley and Stämpfli (1949, Fig. 13) by integration of experimentally measured longitudinal currents. Because of the cusps, the action potential is propagated along the axon with a slight cyclic change of shape, depending on the instantaneous position of the impulse relative to the nodes. Since the values of t used in plotting Fig. 2 were not synchronized with the advance of the impulse past successive nodes, each curve has a slightly different shape.

Fig. 3 shows the same computed data plotted as *temporal* action potential curves (V against t) at various points along the fiber. At the left are plotted curves for the node positions only. The wave form becomes nearly uniform 3 or 4 nodes away from the site of stimulation. At the right, to show how the action potential shape changes cyclically in the internodal regions, curves are plotted for points a quarter of an internode apart, on an expanded time scale. The changes of shape will be discussed in the next section.

As the action potential travels away from the origin, its peak height at the nodes approaches a constant value of 106.58 mv. If the times of peak values in V_j are plotted against node position in an (x, t) plane, these points lie on a straight line from node 1 to the last node reached by the peak before computation stopped—this is (with one exception, see below) node 3 to 6, depending on the stimulus strength. The conduction velocity, calculated from the slope of this line, is the same in all cases: 11.9048 m/sec. Since results are printed out for t increments of 0.024 msec., this velocity represents a conduction time of the peak from node to node equal to exactly 7 of these t increments. A better method of calculating velocity, with a finer time resolution, is obtained by first interpolating linearly to find the time at which $V = 50$ mv during the rising phase at each node, and then calculating the conduction

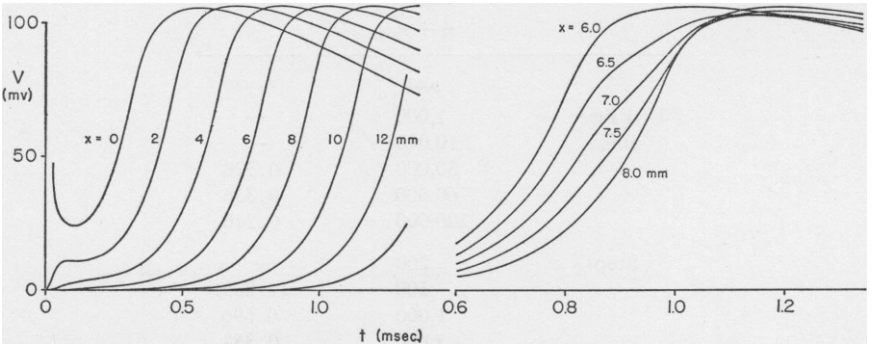

FIGURE 3 Same stimulus as in Fig. 2.
Left: Temporal action potential curves at nodes only, with x values as labeled.
Right: Same, but shown for several positions between two nodes. Steepness of rising phase is less in internodal region, and separate humps due to the two adjacent action potential peaks are visible.

time between each neighboring pair of nodes. The velocity calculated in this way converges, with increasing node number, to a value of 11.90 ± 0.01 m/sec. The close agreement of this value with the figure obtained from the slope in the (x, t) plane is probably accidental; a different choice of values of time to print out might have made it worse.

This value of conduction velocity computed for 6.3°C compares reasonably well with the experimental measurement by Tasaki and Fujita (1948) who obtained about 10 m/sec. for toad axons at 6°C.

Table II shows the stimulus amplitudes (I_p) tried and the corresponding latencies. The latency was taken as defined by the intersection of the above mentioned straight line through the peaks in the (x, t) plane with the line $x = 0$. (This did not always coincide with the actual time of the peak at node 0, where the impulse arose.)

The approach to constant values of spike height and conduction velocity occurs as follows. For 0.01 msec. pulses, the final value of the spike height is approached

from below for the 30,000 $\mu\mu$a stimulus, but from above for 60,000 and 200,000 $\mu\mu$a. The velocity at the 50 mv level of the rising phase is approached from above for 30,000 and from below for 60,000 and 200,000 $\mu\mu$a. Thus the larger action potentials have smaller velocities. (A similar result occurs for the step stimulus.) This relation is the opposite to that observed experimentally in decremental conduction, in which the spike height and conduction velocity, instead of approaching constant limits, both decrease together until the impulse is extinguished (Lorente de

TABLE II

Wave form	Effective stimulus amplitude $\frac{r_1 I_p}{r_1 + r_2}$	Latency
	$\mu\mu a$	*msec.*
0.01 msec. pulse	1,000	—
	10,000	—
	30,000	0.528
	60,000	0.336
	200,000	0.240
Step	200	—
	500	(1.200)
	1,000	0.696
	5,000	0.384
	20,000	0.264

Nó and Condouris, 1959). For the 200,000 $\mu\mu$a, 0.01 msec., stimulus pulse, which was at least 7 times threshold, the spike height was increased by only 0.24 per cent at node 1 (2 mm away from the electrode); for the 20,000 $\mu\mu$a step (at least 40 times threshold) by only 0.075 per cent. The corresponding decreases in velocity below normal were 12.9 per cent and 15.0 per cent between nodes 1 and 2 and only 1.7 per cent and 1.95 per cent between nodes 2 and 3.

A dash in the last column of Table II indicates that the stimulus was below threshold. The latency value in parentheses belongs to the exceptional case referred to above, in which the stimulus was very near threshold and the latency so long that the peak had reached only node 1 by the end of the run. In this case a line with the same slope as used for all the other cases was drawn through the point at node 1 to obtain the latency. This case shows that if the latencies become too long, the duration and cost of the computer runs required to measure threshold accurately can be greatly increased.

From the values given in Table II can be plotted strength-latency curves having the same general shape as the experimental curves of Tasaki and Fujita (1948) in toad and of Hodler, Stämpfli, and Tasaki (1952) in frog axons.

COMPARISON WITH SALTATORY CONDUCTION EVIDENCE

These computations agree in many details with the experimental data accumulated during the controversy, a decade ago, over saltatory conduction in myelinated axons. As summarized by Stämpfli (1954), these data show "discontinuities" in longitudinal action currents and in action potentials, which will be described in more detail below.

The longitudinal external current in the equivalent circuit is equal to $(\partial V/\partial x)/(r_1 + r_2)$. Equation (8) shows that there is a discontinuity in this current at each node, equal to the nodal membrane current; within each internode the longitudinal current is continuous. Experimental measurements by Huxley and Stämpfli (1949, Fig. 7) of longitudinal current at different points along frog axons at 18–20°C show that the time of occurrence of the peak of the longitudinal action current increases only slightly within each internode (about 0.02 msec., with a considerable scatter of points), but jumps to a new value in crossing the node. The new peak time is of course greater than the peak time at the beginning of the previous node by the node-to-node conduction time of the impulse (about 0.1 msec.). The peak longitudinal current value, on the other hand, falls nearly linearly from 2.5 to 1.5 mμa along the internode in the direction of conduction; then, as the node is crossed, jumps back to the higher value.

In comparison, computed curves of longitudinal current for a uniformly propagated impulse, in which the partial derivative $\partial V/\partial x$ is approximated by a difference ratio, resemble the experimental curves of Huxley and Stämpfli in shape. The peak time increases only 0.015 msec. along one internode, while the node-to-node conduction time is 0.168 msec. (These times should be divided by 2 or 2.5 to correct for the difference of temperature.) The peak value of longitudinal current falls from 2.6 to 1.5 mμa along one internode. These computed figures are thus in reasonably good agreement with experiment.

The experimental measurements which most nearly resemble the computed temporal action potential curves of Fig. 3 (right) are those of Hodler, Stämpfli, and Tasaki (1952; see also Laporte, 1951, and Stämpfli and Zotterman, 1951). They recorded the potential at the point on the outside of a single fiber where it emerged from a Ringer-filled glass capillary, moving the fiber in the capillary to record at different points. Their reference potential was at the other end of the capillary, and an injured end lay within the capillary. They assumed that the recorded potential was a constant fraction of the potential between the outside medium and the axoplasm; *i.e.*, of V. Their peak potentials did "not vary appreciably as a function of distance along the fiber." In comparison, the computed peak potentials fall from 106.58 mv at the nodes to 102.86 mv midway between two adjacent nodes. Such a decrease of only 3.5 per cent would probably be indistinguishable experimentally from the effects of non-uniformity of the fiber.

The "steepness" or maximum rate of rise of the action potential recorded experimentally by these authors in the middle of an internode was only about one-half that at the nodes. The computed values change from 461.2 v/sec. at the nodes to 292.2 v/sec. at a point five-eights of the way from one node to the next in the direction of propagation, a ratio of 1/1.6.

An examination of the curves in Fig. 3 (right) shows that there are two local maxima in slope, and the point of the absolute maximum slope jumps from one of these points to the other as x increases. The internodal action potential curve may be thought of as a superposition of two action potentials picked up at the point of recording by electrotonic spread from the adjacent nodes. This interpretation of the apparently irregular shape of the internodal temporal action potentials can be seen rather more clearly in the computed curves than in the experimental curves cited above, perhaps because of axon non-uniformity and the somewhat different conditions of measurement in the latter.

Dr. K. S. Cole suggested making these computations. Dr. Walter Gautschi, formerly of the National Bureau of Standards, worked out the numerical method for solving the equations on the computer. Mr. Alfred Beam of NBS wrote the program and carried out the computations there. Dr. F. A. Dodge made several constructive criticisms of the manuscript.

Received for publication, August 29, 1961

REFERENCES

COLE, K. S., ANTOSIEWICZ, H. A., and RABINOWITZ, P., 1955, Automatic computation of nerve excitation, *J. Soc. Ind. Appl. Math.*, **3**, 153.

DODGE, F. A., 1961, A quantitative description of membrane excitation at a node of Ranvier, paper given at 5th Annual Meeting of the Biophysical Society, St. Louis.

DODGE, F. A., and FRANKENHAEUSER, B., 1958, Membrane currents in isolated frog nerve fibre under voltage clamp conditions, *J. Physiol.*, **143**, 76.

FITZHUGH, R., 1960, Thresholds and plateaus in the Hodgkin-Huxley nerve equations, *J. Gen. Physiol.*, **43**, 867.

FITZHUGH, R., 1961, Impulses and physiological states in theoretical models of nerve membrane, *Biophysic. J.*, **1**, 445.

FITZHUGH, R., and Antosiewicz, H. A., 1959, Automatic computation of nerve excitation—detailed corrections and additions, *J. Soc. Ind. Appl. Math.*, **7**, 447.

GEORGE, E. P., 1960, Action potentials in active tissue with delayed potassium permeability, *Nature*, **186**, 889.

HODGKIN, A. L., and HUXLEY, A. F., 1952, A quantitative description of membrane current and its application to conduction and excitation in nerve, *J. Physiol.*, **117**, 500.

HODLER, J., STÄMPFLI, R., and TASAKI, I., 1952, Role of potential wave spreading along myelinated nerve in excitation and conduction, *Am. J. Physiol.*, **170**, 375.

HUXLEY, A. F., 1959*a*, Ion movements during nerve activity, *Ann. New York Acad. Sc.*, **81**, 221.

HUXLEY, A. F., 1959*b*, Can a nerve propagate a subthreshold disturbance?, *J. Physiol.*, **148**, 80P.

HUXLEY, A. F., and STAMPFLI, R., 1949, Evidence for saltatory conduction in peripheral myelinated nerve fibres, *J. Physiol.*, **108**, 315.

LAPORTE, Y., 1951, Continuous conduction of impulses in peripheral myelinated nerve fibers, *J. Gen. Physiol.*, **35**, 343.

LORENTE DE NÓ, R., and CONDOURIS, G. A., 1959, Decremental conduction in peripheral nerve. Integration of stimuli in the neuron, *Proc. Nat. Acad. Sc.*, **45**, 592.

MILNE, W. E., 1953, Numerical solution of differential equations, New York, John Wiley & Sons, Inc.

SCARBOROUGH, J. B., 1958, Numerical Mathematical Analysis, Baltimore, Johns Hopkins Press, 4th edition.

STÄMPFLI, R., 1954, Saltatory conduction in nerve, *Physiol. Rev.*, **34**, 101.

STÄMPFLI, R., and ZOTTERMAN, Y., 1951, Nachweis der saltatorischen Erregungsleitung am intakten Nervenstamm, *Helv. Physiol. et Pharmacol. Acta*, **9**, 208.

TASAKI, I., 1955, New measurements of the capacity and the resistance of the myelin sheath and the nodal membrane of the isolated frog nerve fiber, *Am. J. Physiol.*, **181**, 639.

TASAKI, I., and FRANK, K., 1955, Measurement of the action potential of myelinated nerve fiber, *Am. J. Physiol.*, **182**, 572.

TASAKI, I., and FREYGANG, W. H., 1955, The parallelism between the action potential, action current, and membrane resistance at a node of Ranvier, *J. Gen. Physiol.*, **39**, 211.

TASAKI, I., and FUJITA, M., 1948, Action currents of single nerve fibers as modified by temperature changes, *J. Neurophysiol.*, **11**, 311.